Electrochimica Acta 56 (2011) 4007–4014

Contents lists available at ScienceDirect

Electrochimica Acta

journal homepage: www.elsevier.com/locate/electacta

Photoinducedly electrochemical preparation of Prussian blue film and electrochemical modification of the film with cetyltrimethylammonium cation

Shou-Qing Liu [a,*], Hua Li [a], Wei-Hui Sun [a], Xiao-Mei Wang [a], Zhi-Gang Chen [a], Jing-Juan Xu [b], Huang-Xian Ju [b], Hong-Yuan Chen [b]

[a] Key Laboratory of Environmental Functional Materials of Jiangsu Province, College of Chemistry and Bioengineering, Suzhou University of Science and Technology, Suzhou 215009, China
[b] Key Laboratory of Analytical Chemistry for Life Science, Ministry of Education, Nanjing University, Nanjing 210093, China

ARTICLE INFO

Article history:
Received 26 December 2010
Received in revised form 27 January 2011
Accepted 1 February 2011
Available online 17 February 2011

Keywords:
Photoinduced
Sodium nitroprusside
Prussian blue
Cetyltrimethylammonium bromide
Electrochemistry

ABSTRACT

This work presents a photoinducedly electrochemical preparation of Prussian blue from a single sodium nitroprusside and insertion of cetyltrimethylammonium cations into Prussian blue as counter ions. The product of photoinducedly electrochemical reactions has a couple of voltammetric peaks at $E^\circ = 0.266$ V in 0.2 mol l^{-1} KCl solution, the measurements of X-ray powder diffraction and FT-IR spectroscopy show that it is Prussian blue (PB). The formation mechanism of a pre-photochemical reaction and subsequent electrochemical reaction is suggested. The cyclic voltammetric treatment of the freshly as-prepared PB film in 1.0 mmol l^{-1} cetyltrimethylammonium (CTA) bromide solution leads to the insertion of cetyltrimethylammonium cations into the channels of Prussian blue, which substitutes for potassium ions as counter ions in Prussian blue. The Prussian blue containing CTA counter ions shows two couples of voltammetric peaks at $E^\circ = -0.106$ V and $E^\circ = 0.249$ V in 0.2 mol l^{-1} KCl solution containing 1.0 mmol l^{-1} cetyltrimethylammonium bromide. Compared with the electrochemical behaviors of $KFeFe(CN)_6$ in 0.1 mol l^{-1} KOH alkali solution, $CTAFeFe(CN)_6$ shows relatively durable voltammetric currents due to the hydrophobic effects of cetyltrimethylammonium. The diffusion coefficients for CTA and potassium cations were estimated to be D_{CTA} 1.25×10^{-12} cm^2 s^{-1}, D_K 2.59×10^{-12} cm^2 s^{-1}, respectively. The peak current of electro-catalytic oxidization on hydrogen peroxide showed a linear dependence from 6.59×10^{-6} to 2.20×10^{-4} mol l^{-1} with $R = 0.99947$ ($n = 8$). The linear regression equation was I_p (mA) = 0.82949 + 0.00594C (μmol l^{-1}) with errors of $\pm 7.92833 \times 10^{-5}$ for the slope and ±0.01085 for the intercept with the detection limit of 1.46×10^{-6} mol l^{-1}. Thus, it is expected to find its application in neutral or weak alkali medium for biosensors.

1. Introduction

Prussian blue (PB) is a prototype of mixed-valence compounds with composition of metal hexcayanoferrate (MHCF) or pentacyanonitrosylferrate (where the anion hexcayanoferrate is substituted with pentacyanonitrosylferrate, commonly known as nitroprusside). After Neff [1] and Bocarsly [2] first reported the electrochemical studies on Prussian blue and metal metallocyanide ($Fe(CN)_6^{3-}$, $Ru(CN)_6^{3-}$, $Mn(CN)_6^{3-}$, $[Fe(CN)_{6-x}L_x]^{n-}$, L = H_2O, NO, histidine, 1,2-cyclohexyldiamine), respectively, these species have arisen considerable interests due to their attractive properties such as electrocatalysis [3–8], electrochromism [9–12], ion-exchange [13–17], photomagnetism [18,19], photoelectrochemical switch effect [20] and magnetoresistance effect [21]. On the basis of these properties, some biosensors [22–29], electrochromic devices [30–32], ion-sensing [33–37], and optical sensing devices [38,39] were developed. Especially, Prussian blue is often used as an artificial enzyme for the fabrication of biosensors due to its response to hydrogen peroxide released from the reaction of glucose with dioxygen in the presence of glucose oxidase under low potential conditions. This low potential could limit effectively the interference from the coexisting substances [25] such as dopamine, ascorbic acid and uric acid because these substances are easily oxidized at high potentials. Unfortunately, Prussian blue is unstable at pH > 5.0 solutions [40,41] whereas the pH value of human blood is 7.2–7.4. And Prussian blue can be dissolved during the voltammetric cycles even in neutral aqueous solutions [42] due to its high sensitivity to hydroxy, which decreases the lifetime of biosensors. Therefore, it is necessary to extend the pH range of Prussian blue and improve its stability for preparing biosensors.

The recent studies demonstrated that surfactant treatment of metal hexacyanoferrate compounds is very effective in improv-

* Corresponding author. Fax: +86 512 69209055.
E-mail address: shouqing_liu@hotmail.com (S.-Q. Liu).

0013-4686/$ – see front matter © 2011 Elsevier Ltd. All rights reserved.
doi:10.1016/j.electacta.2011.02.012

ing their electrochemical stability. Vittal and coworkers first researched the influence of cetyltrimethylammonium bromide (CTAB, cetyltrimethylammonium cation was denoted as CTA), a cationic surfactant often used in electrochemistry, on the electrochemical behaviors of Prussian blue [43–45]. And thereafter a few papers presented the influence of CTAB, polyvinyl alcohol, polyvinyl pyrrolidone, polyallylamine hydrochloride, polydiallyldimethyldiammonium chloride and polystyrene sulfonate on the stability of PB and its analogues nickel or cobalt hexacyanoferrate [46–49]. Polyelectrolyte semiconductor nanoparticle composite films were prepared successfully by layer-layer self-assembly method for improving stability [50]. However, less well known is how surfactant enhances the electrochemical stability of MHCF films, whether surfactant enters into the channel of the metal hexacyanoferrate compounds, and how much the content of surfactant in the metal hexacyanoferrate compounds is (if CTA in the films). A point of view is accepted commonly that the structure of MHCF can affect the electrochemical behavior and stability, thus it is expected to obtain the structural information on surfactant improving the PB stability.

Previously, we reported the electrochemical behaviors of nanosized Prussian blue [51], LaHCF [52], and ZrHCF [53]. In the present work, we focus on a new preparation method of PB film on a sheet of indium tin oxide (ITO) transparent conductive glass by voltammetric sweeps in a single nitroprusside solution under white light irradiation. It is expected to be helpful to understand the enhanced stability of PB film after being treated electrochemically in CTAB solution. In order to realize the goal, an as-prepared PB film was scanned electrochemically in an aqueous CTAB solution and the film was characterized by cyclic voltammetry, Fourier transform infrared spectroscopy (FT-IR), X-ray powder diffraction (XRD) measurements, scanning electronic microscopy (SEM) and transmission electron microscope (TEM).

2. Experimental

2.1. Materials

The chemicals, KCl, $K_3Fe(CN)_6$ and $(NH_4)_2Fe(SO_4)_2$ (purchased from Beijing Chemical Reagent Factory, China), are of analytical reagent grade and used as received. The content of sodium nitroprusside (purchased from Guangzhou Chemical Reagent Factory, China) is more than 98.00%. The purity of cetyltrimethylammonium bromide (purchased from Shanghai Linfeng Chemical Reagent Co., Ltd., China), is more than 99.9%. The water used in experiments was purified with a Milli-Q system with a resistivity higher than 18.2 MΩ cm. All solutions were prepared with the deionized water.

2.2. Apparatus

Cyclic voltammetry was performed using a CHI660C electrochemical workstation (CH Instrument Company, TX, USA). The electrochemical experiments were conducted in a conventional three-electrode system. An ITO conductive glass sheet electrode was used as working electrode with resistance 11.4 Ω/sq. The ITO glass was tailored into a square with 1.0 cm wide and 2.0 cm long, and the square ITO glass was wrapped with a piece of insulation tape to obtain an unchanged working area of 1.0 cm × 1.0 cm. Thus, the interface between ITO electrode and solution is always equal to 1.0 cm^2 in our experiments. A platinum foil was used as counter electrode and a saturated calomel electrode (SCE) as reference electrode. The photoelectrochemical cell is a 4 cm × 4 cm × 5 cm quartz one and illuminated with a beam of light from 350 W Xe lamp, the diameter for the beam of light is round 2 cm. A water filter of 4 cm length was placed between the light source and the three electrode cell to adsorb infrared irradiation and keep the cell temperature constant. All the experiments were performed under room temperature (25 ± 2 °C). The diffraction powder patterns were measured with X'Pert-Pro MPD X-ray diffractometer, Panalytical, Netherland. The source of X-ray is Cu-K with wavelength 0.154 nm at tube voltage 40 kV and tube current 40 mA. The X-ray was filtered with nickel monochromator. The diffraction patterns measured were compared with standard data in the database offered by Panalytical Company, Netherland. The morphological observation was carried out with transmission electron microscope (TecnaiG220, FEI, USA) and scanning electronic microscopy (Quanta 400 FEG, FEI, USA).

The FT-IR spectra were measured with FT-IR spectrophotometer (Spectrum BX, PerkinElmer Ltd., USA). The optical resolution was 4 cm^{-1}. The samples of Prussian blue synthesized by electrochemistry were scraped off from ITO glass with a scalpel after the electrodes were rinsed with deionic water and dried for XRD, IR, SEM measurements. The mulls of Prussian blue synthesized electrochemically and chemically were supported by KBr.

2.3. Preparation of Prussian blue film

Prussian blue film was prepared as follows: a fresh ITO glass electrode was tailored by the method mentioned according to the desired size, and was washed with deionized water first. And then, it was cleaned with alcohol in an ultrasonic cleaner for 15 min. Finally, it was rinsed thoroughly with deionized water again. If necessary, the above pre-treatment for ITO electrode could be repeated until a clean ITO electrode was obtained. Such an ITO electrode was immersed in a single sodium nitroprusside solution for electrochemical preparation of Prussian blue film under irradiation. The concentration of sodium nitroprusside solution was 1.0×10^{-2} mol l^{-1} with 0.20 mol l^{-1} KCl supporting electrolyte.

A freshly as-prepared PB film was scanned immediately in 1.0 mmol l^{-1} CTAB solution to characterize the influence of CTAB on PB film. The lights of wavelength 380 nm and 460 nm were obtained by a 380-cutoff filter that allows the light with the wavelength λ > 380 nm to pass, and a 460-cutoff filter that allows the light with the wavelength λ > 460 nm to pass, respectively.

3. Results and discussion

3.1. Photoinducedly electrochemical preparation

A clean ITO electrode was immersed in a 1.0×10^{-2} mol l^{-1} nitroprusside solution containing 0.20 mol l^{-1} KCl pH 6.50 supporting electrolyte, then cyclic voltammetric sweeps were performed between −0.40 V and 0.60 V at a scan rate of 50.0 mV s^{-1}, the resulting cyclic voltammograms under irradiation were very different from those in dark as denoted in Fig. 1. Under illumination the voltammetric peak currents increased gradually with cyclic time whereas the voltammetric ones kept almost unchanged in the same solution in dark, suggesting the illumination induces the electrochemical reaction.

That the current increased gradually but not immediately under illumination means the current is electrochemical reaction current but is not photocurrent. The resulting film under illumination is blue seen with naked eyes, the cyclic voltammograms of the blue film electrode in 0.2 mol l^{-1} KCl supporting electrolyte were shown in Fig. 2. From the Figure a couple of voltammetric peaks can been seen with an anodic peak potential at 0.300 V versus SCE and a cathodic peak potential at 0.232 V versus SCE (the formal redox potential $E^{\circ} = (E_{pa} + E_{pc})/2 = 0.266$ V), the potential difference of peak to peak is 68.0 mV (similar to one [45] reported by Pillai where the potential difference for Prussian blue is 80 mV), showing a non-surface control kinetic characteristics. Further studies

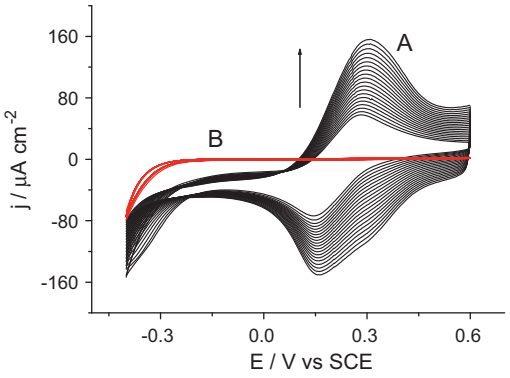

Fig. 1. Cyclic voltammograms of an ITO electrode in a single 1.0×10^{-2} mol l^{-1} nitroprusside solution containing 0.20 mol l^{-1} KCl supporting electrolyte at a scan rate of 50 mV s^{-1} for 20 cycles: (A) under irradiation and (B) in dark.

showed the blue film can be also obtained by cyclic voltammetry in nitroprusside solution after the solution was illuminated for 15 min. In this case the peak potentials of the resulting film for the anode and the cathode were the exact same as those under in situ illumination, suggesting the product in both cases is the same. However, the currents of voltammetric peaks cannot be obtained if a clean ITO electrode was scanned in a fresh nitroprusside solution without illumination. Moreover, the peak currents increase with the scanning cycles under irradiation of light with wavelength 380 nm whereas the currents kept almost unchanged under irradiation of light with wavelength 460 nm (see supporting materials). Thus, $[Fe(CN)_5H_2O]^{2-}$, an intermediate, was formed under irradiation of light with wavelength 360 nm [54], and it might be transferred further to Prussian blue during the potential sweep.

3.2. Stability of PB film in KCl solution

To examine the stability of the freshly prepared blue film, the electrode was scanned continuously for 20 cycles (Fig. 3) in 0.20 mol l^{-1} pH 6.50 KCl solution. The results showed that the peak current declined by 87.5% for the anodic peak, 86.1% for the cathodic peak, which indicates the PB film is not very stable in the nearly neutral medium. Therefore, the stability needs to improve.

3.3. Electrochemical treatment in CTAB solution

In order to improve the stability of the film, the as-prepared PB film on ITO electrode was immersed in 1.0 mmol l^{-1} CTAB solution containing 0.2 mol l^{-1} KCl electrolyte for 20 voltammetric cycles. The obtained voltammograms for 20 cycles were shown in Fig. 4.

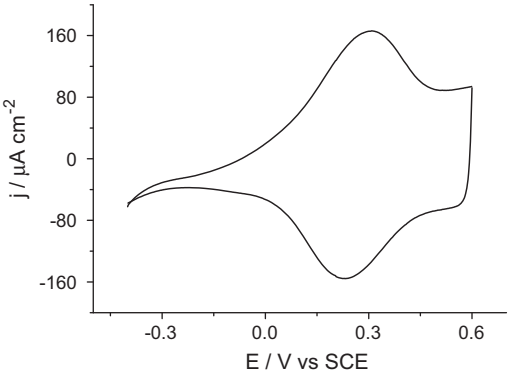

Fig. 2. Cyclic voltammograms of the as-prepared electrode formed under illumination in 0.2 mol l^{-1} KCl supporting electrolyte. The scan rate was 50 mV s^{-1}, the potential range was from −0.40 V to 0.60 V.

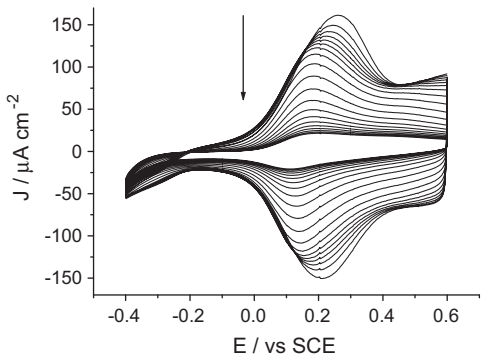

Fig. 3. Cyclic voltammograms of the as-prepared PB film in 0.20 mol l^{-1} KCl solution for 20 cycles. The scan rate: 50 mV s^{-1}; potential range: −0.40 V to +0.60 V versus SCE.

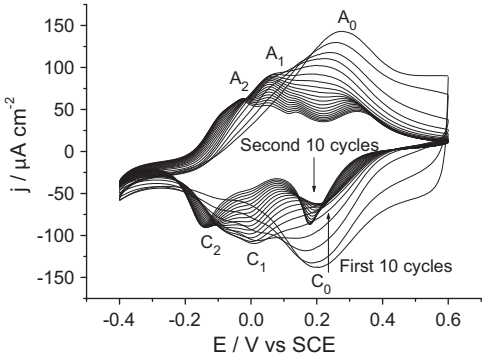

Fig. 4. Cyclic voltammograms of the as-prepared PB film on ITO electrode in 1.0 mmol l^{-1} CTAB solution containing 0.2 mol l^{-1} KCl supporting electrolyte. The scan rate was 50 mV s^{-1}, the potential range was from −0.40 V to 0.60 V.

Fig. 4 shows the currents declined at the couple of peaks A_0 and C_0 during the first 10 cycles, and then peak C_0 started to become bigger and bigger at the eleventh cycle. At the fifth cycle the couple of peaks A_1 and C_1 appeared obviously, and subsequently the couple of peaks became smaller and smaller or even disappeared. At the tenth cycle a new couple of peaks A_2 and C_2 started to appear, the couple of peaks A_2 and C_2 became stable and increased gradually during the sequential cycles. At the end two couples of voltammetric peaks appeared as shown in Fig. 5. For one couple of cyclic voltammetric peaks, the potential of anodic peak is

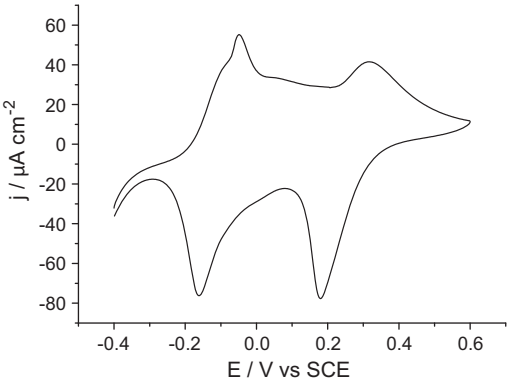

Fig. 5. Cyclic voltammetric curves of CTA-PB film on ITO electrode in 0.2 mol l^{-1} KCl solution. The scan rate was 50 mV s^{-1}, the potential range was from −0.40 V to 0.60 V.

Table 1
Current data of PB film.

Current	PB film[a]	PB film[b]	CTA-PB film[c]
I_{pa} (μA)	165.7	22.2	97.6
I_{pc} (μA)	−157.6	−20.5	−153.6

[a] PB film: currents of the freshly prepared PB film in 0.2 mol l^{-1} KCl solution.
[b] PB film: currents after cyclic voltammetry in 0.2 mol l^{-1} KCl solution for 20 cycles.
[c] CTA-PB film: sum of two peak currents after cyclic voltammetry in 0.2 mol l^{-1} KCl + 1.0 mmol l^{-1} CTAB solution for 20 cycles.

−0.047 V and potential of cathodic peak is −0.165 V, the formal redox potential E° = −0.106 V in 0.2 mol l^{-1} KCl solution containing 1.0 mmol l^{-1} CTAB, the potential difference of peak to peak is 0.118 V. For the other couple of cyclic voltammetric peaks, the potentials of anodic and cathodic peaks are 0.318 V and 0.180 V, respectively, the formal redox potential E° = 0.249 V in 0.2 mol l^{-1} KCl solution containing 1.0 mmol l^{-1} CTAB, the potential difference of peak to peak is 0.138 V.

Compared with that in 0.2 mol l^{-1} KCl solution (Fig. 3), the stability of the film in 1.0 mmol l^{-1} CTA solution was improved greatly. The current data of a freshly prepared PB film electrode, ones after it was scanned in 0.20 mol l^{-1} KCl solution, and in 1.0 mmol l^{-1} CTAB + 0.20 mol l^{-1} KCl solution for 20 cycles, were listed in Table 1 (the PB that was treated electrochemically in CTAB aqueous solution was denoted as CTA-PB).

Data in Table 1 show without doubt the CTA-PB film electrode is more stable than the freshly Prussian blue.

3.4. FT-IR characterization

3.4.1. Studies on IR spectra of synthesized PB and electro-synthesized PB

In order to identify the composition of the blue film, FT-IR spectra of the species from both chemically and photoinducedly electrochemical syntheses were measured. The resulting spectra are similar to each other as shown in Fig. 6 and displayed the unique characteristic peak of Prussian blue. The absorption at 2076 cm^{-1} is assigned to T_{1u} CN stretching vibration, 598 cm^{-1} and 498 cm^{-1} assigned to metal–carbon–nitrogen bending mode [9]. The absorptions at 3430 cm^{-1} and 1631 cm^{-1} assigned to the stretching and bending modes of interstitial water in PB lattice channel, respectively.

The absorptions at 2363 cm^{-1}, 1391 cm^{-1} and 677 cm^{-1} are assigned to the anti-symmetric stretching vibration, symmetric stretching vibration, and bending mode of carbon dioxygen, respectively. A small absorption at 1940 cm^{-1} indicates the presence of coprecipitated nitroprusside ions [55], which is similar to that of

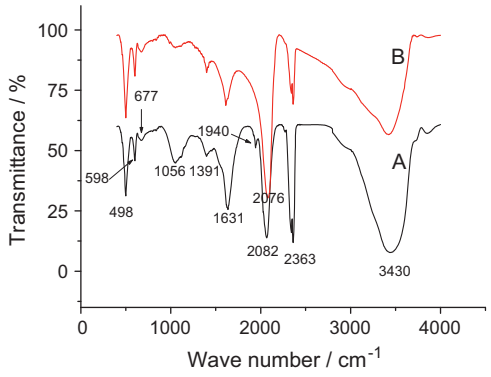

Fig. 6. FT-IR spectra for Prussian blue: (A) photoinducedly electrochemical synthesis and (B) chemical synthesis.

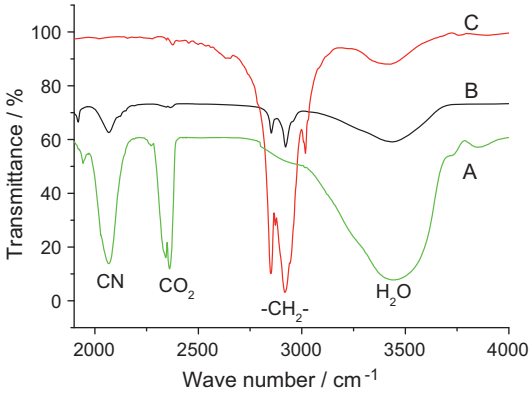

Fig. 7. FT-IR spectra of PB film (A), CTA-PB film treated in CTAB aqueous solution (B) and solid CTAB (C).

Prussian blue (where ferricyanide ions were coprecipitated in PB) [9].

Because photolysis of nitroprusside in aqueous solution with light of wavelength 340–430 nm forms $[Fe(CN)_5H_2O]^{2-}$ [54], and the irradiation of wavelength λ = 460 nm did not lead to the increase of peak current in our diagnostic voltammetric experiment (see supporting materials), the mechanism of the overall reactions is suggested as follows:

$$\text{Photochemical reaction}: Fe^{III}(CN)_5NO^{-} + H_2O + h\nu \rightarrow [Fe^{III}(CN)_5H_2O]^{2-} + NO \quad (1)$$

$$\text{Electrochemical reaction}: 2[Fe^{III}(CN)_5H_2O]^{2-} + K^{+} + e^{-} \rightarrow K[Fe^{III}Fe^{II}(CN)_6]\cdot nH_2O + 4CN^{-} \quad (2)$$

Here the species NO· is first released on irradiation [54–60], and then, the "soluble" [48,49,61] Prussian blue containing potassium ions is formed due to the presence of an excess of potassium ions as supporting electrolyte in solution.

3.5. Studies on IR spectra of CTA-PB

To elucidate the structure and composition of the film after it being scanned in CTAB solution, the infrared spectroscopic measurements were performed, the obtained IR spectra of CTA-PB, PB and pure CTAB were shown in Fig. 7. The two intense bands around 2920 cm^{-1} and 2852 cm^{-1}, in both CTAB and CTA-PB, were assigned to asymmetric and symmetric stretching vibration [62] of C–CH_2 from the methylene chain, respectively. The assignments of stretching vibrations from both CH_2 in CTA and CN in PB were listed in Table 2. The finding of the methylene chain in PB film treated electrochemically in CTAB aqueous solution confirmed the presence of CTA cations in the film by comparison of IR data in Table 2. The quantitative analysis from IR spectrum of CTA-PB film has shown that the intensity ratio of peaks ν_{CH_2} to ν_{CN} is close to 1:1, which is in agreement with that from $CTAFe^{II}Fe^{III}(CN)_6$ film (see supporting materials), whereas the ratio in $(CTA)_3Fe(CN)_6$ is

Table 2
IR band assignments of the methylene chain CH_2 stretching vibrations for CTAB and CN stretching vibration for PB and intensity ratio.

Species	CH_2 stretching vibration (cm^{-1})	CN stretching vibration (cm^{-1})	Intensity ratio of peak ν_{CH_2} to ν_{CN}
PB	–	2076	–
CTAB	2920, 2852	–	–
CTA-PB	2920, 2852	2076	1:1

close to 3:1. The relative ratios confirm that the molar ratio of fericyanide to cetyltrimethylammonium in CTA-PB is equal to 1:1. Moreover, Fe(II), CATB and $Fe(CN)_6^{3-}$ were mixed to result in a blue species, the XRD pattern of the species is consistent with that of PB (see the next section and supporting materials). Thus, CTA ions were inserted to Prussian blue and work as counter ions. The electrochemical reaction of the soluble PB in aqueous CTAB solution can be shown as follows:

$$KFe^{II}Fe^{III}(CN)_6 + CTA^+ + e^- \rightarrow CTAKFe^{II}Fe^{II}(CN)_6 \quad (3)$$

$$CTAKFe^{II}Fe^{II}(CN)_6 - e^- \rightarrow CTAFe^{II}Fe^{III}(CN)_6 + K^+ \quad (4)$$

$CATFe^{II}Fe^{III}(CN)_6$ was formed by reactions (3) and (4).

It is reasonable that CTA cations entered into the channels of Prussian blue as counter ions during the potential sweeps, because Prussian blue needs chargedly positive ions to maintain the electroneutrality when it is reduced to Everitt's salt. The couple of peaks A1 and C1 in Fig. 6 could be assigned to the intermediate or transition state during the electrochemical sweeps. In the case of CTA cations that worked as counter ions in PB film the chemical surroundings of electroactive components have been changed, so a new couple of peaks appeared at $E^\circ = -0.106$ V. In fact, the counter ions in Prussian blue film have major effects on peak potentials. For example, the peak potentials of PB film in aqueous NaCl solution are very different from those in KCl electrolyte [48].

3.6. XRD characterization

Prussian blue was synthesized from the starting materials both $K_3Fe(CN)_6$ and $(NH_4)_2Fe(SO_4)_2$. They were mixed equivalently, the classic volume of each is 30 mL in the concentration of 1.0×10^{-2} mol l^{-1} in the presence of 0.2 mol l^{-1} KCl. It should be noted that the PB synthesized chemically is under conditions in an excess of potassium ion, which is similar to the case of the photoinducedly electrochemical synthesis of the blue film. Thus it ensures the formation of the soluble Prussian blue containing potassium ions [48,49].

The blue powder (A) photoinducedly electro-synthesized, Prussian blue (B) synthesized chemically, and CTA-PB (C) (the synthetic procedure can be seen in supporting materials) were detected with X-ray powder diffraction. The resulting diffraction patterns were shown in Fig. 8 as follows.

The XRD measurements showed these three species possess the similar diffraction pattern, the diffraction angle positions of 2θ are in very good agreement with data of JCPDS card of Prussian blue as listed in Table 3. Thus, the data of XRD confirmed the product of photoinducedly electrochemical reaction is Prussian blue and CTA cations were inserted into the PB channels.

3.7. Film morphological observations

The morphology of the as-prepared PB sample was characterized by SEM. Fig. 9 shows the imagines of the as-prepared PB particles amplified by 20000 times before (a) and after (b) it was

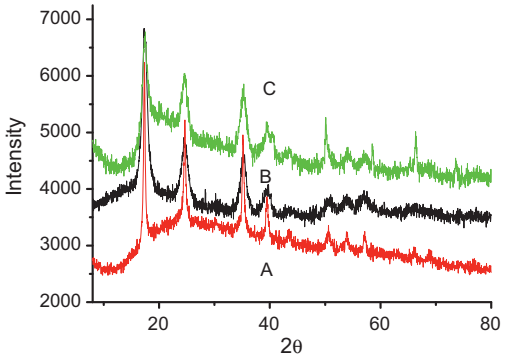

Fig. 8. X-ray powder diffraction patterns of Prussian blue: (A) photoinducedly electrochemical synthesis, (B) chemical synthesis and (C) synthesis from the mixture of Fe(II), CATB and $Fe(CN)_6^{3-}$.

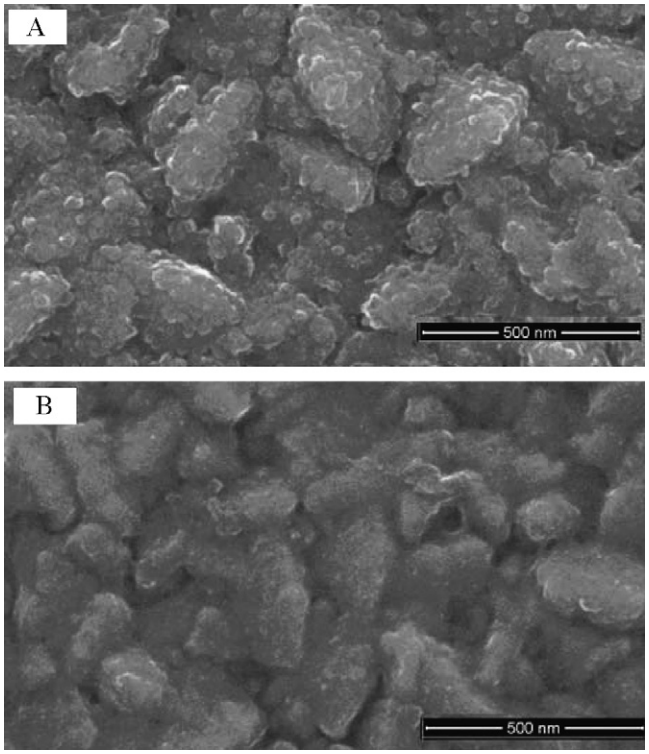

Fig. 9. SEM patterns of the as-prepared PB samples before electrochemical treatment (a), and after electrochemical treatment in 1.0 mmol l^{-1} CTAB solution (b).

treated electrochemically in 1.0 mmol l^{-1} CTAB solution. The difference between (a) and (b) in Fig. 9 is that the small convex shapes like bean can be clearly seen from the freshly prepared PB film, whereas they became flat after the film was scanned electrochemically in CTAB solution. Compared with PB film prepared by the traditional electrochemical method, the present PB film is more

Table 3
Data of XRD for Prussian blue.

PB	2θ (°)	17.39	24.66	35.21	39.62	50.62	54.34
	d (Å)	5.09	3.61	2.55	2.27	1.80	1.69
CTA-PB	2θ (°)	17.28	24.66	35.21	39.62	50.11	53.88
	d (Å)	5.13	3.61	2.55	2.27	1.82	1.70
JCPDS	d (Å)	5.10	3.60	2.55	2.28	1.80	1.70
	hkl	100	110	200	210	220	221, 300
	I/I_1	100	32	48	32	14	13

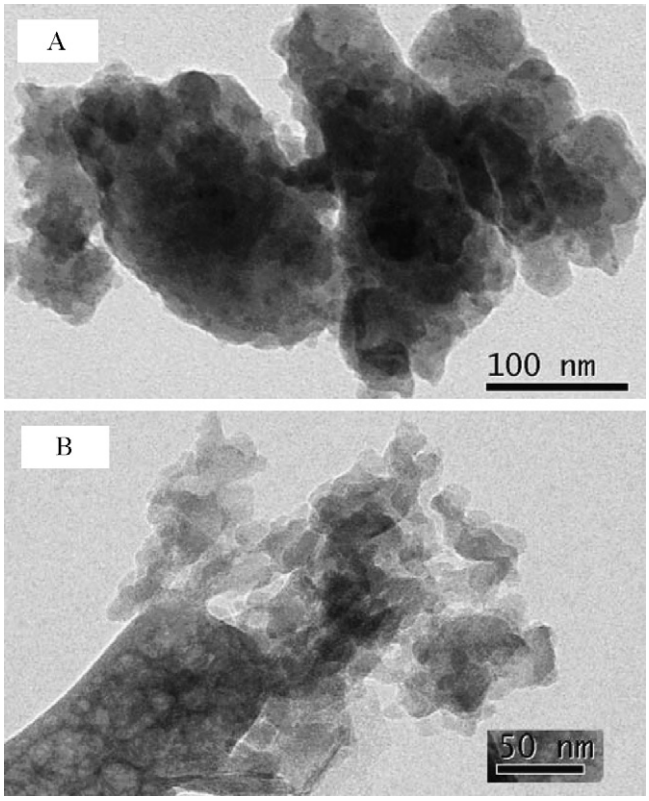

Fig. 10. TEM imagines of PB particles before (a) and after (b) the electrochemical treatment.

uniform. The TEM observations displayed that the small convexes are the nano-particles with the diameter of 20–30 nm as shown in Fig. 10.

3.8. Electrochemical behaviors of CTA-PB film and diffusion coefficients

The obtained CTA-film electrode was immersed in 0.2 mol l^{-1} KCl solution containing 1.0 mmol l^{-1} CTA for the electrochemical characterization at different scan rates, the resulting voltammetric curves were shown in Fig. 11. The corresponding plots of anodic peak currents versus square roots of scan rates were shown in Fig. 12. The figure indicates the anodic peak currents

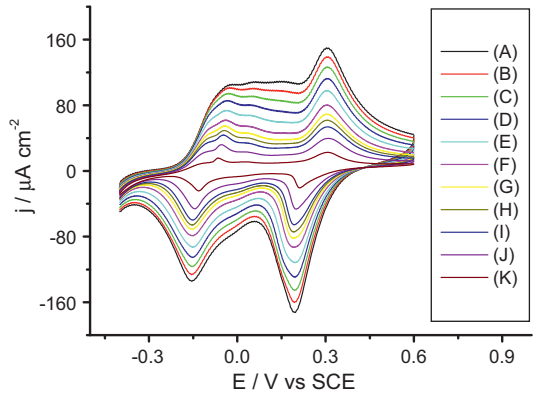

Fig. 11. Cyclic voltammograms of CTA$Fe^{III}Fe^{II}(CN)_6$ in 0.20 mol l^{-1} KCl solution containing 1.0 mmol l^{-1} CTAB at different scan rates: (A) 20.0 mV s^{-1}, (B) 50.0 mV s^{-1}, (C) 80.0 mV s^{-1}, (D) 100.0 mV s^{-1}, (E) 120.0 mV s^{-1}, (F) 150.0 mV s^{-1}, (G) 200.0 mV s^{-1}, (H) 250.0 mV s^{-1}, (I) 300.0 mV s^{-1}, (J) 350.0 mV s^{-1}, and (K) 400.0 mV s^{-1}, respectively.

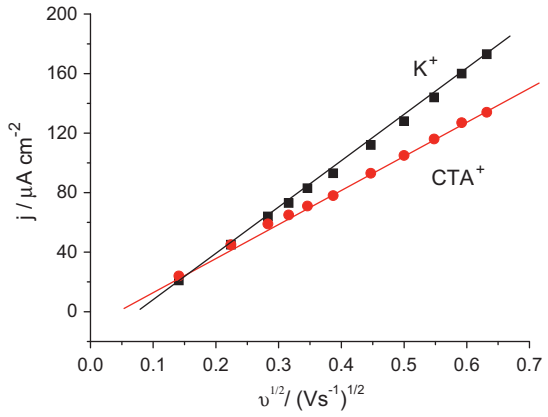

Fig. 12. Relationship between the anodic peak current and the square roots of scan rate.

versus square roots of scan rates have a good linear relationship, the linear correlation coefficient is $R = 0.99938$ for CTA and $R = 0.99949$ for potassium, respectively, suggesting both electrochemical reduction processes are under diffusion control, which is in good agreement with that of Prussian blue [9]. The concentration of PB on ITO surface was estimated to be 1.33×10^{-9} mol cm^{-2} based on $\Gamma = Q/(nFA)$, where Γ is surface coverage in mol cm^{-2}, Q the total Faradaic coulumb, F Faraday constant (96,485 C), A the electrode area (cm^2). The PB concentration or thickness can be controlled by scanning time or cycles. If the molar volume [63] of PB is 677 cm^3 mol^{-1}, the concentration of electroactive component on ITO surface was calculated to be 1.48×10^{-3} mol cm^{-3}. Thus, the peak height is given by the Randles–Sevcik equation [64,65]

$$i_p = 2.69 \times 10^5 n^{3/2} A D^{1/2} C \nu^{1/2} \quad (6)$$

where i_p is the peak current in amperes, n the electron transfer number, A the electrode area in cm^2, D the diffusion coefficient in cm^2 s^{-1}, C the concentration of the electroactive species in mol cm^{-3} and ν the scan rate in V s^{-1}. On the basis of the slope of i_p versus $\nu^{1/2}$ plot in Eq. (6) one can calculate the apparent diffusion coefficient of both CTA and potassium inside the CTA–PB film. For CTA ions, D_{CTA} is 1.25×10^{-12} cm^2 s^{-1} and D_K is 2.59×10^{-12} cm^2 s^{-1} for potassium ions. It is to be noted that the D values obtained are comparable to those obtained for PB film by other methods [66].

3.9. Stability of CTA-PB in alkali medium

The as-prepared CTA$Fe^{III}Fe^{II}(CN)_6$ electrode is very stable, the peak current can still keep even in 0.1 mol l^{-1} KOH electrolyte for 20 potential cycles, the current drop is only 22.5% denoted as Fig. 13. However, the voltammetric peak current of Prussian blue (it was prepared by popular potential sweeps between −0.2 V and 1.0 V for 5 cycles in 1.0 mmol l^{-1} $FeCl_3$ + 1.0 mmol l^{-1} $K_3Fe(CN)_6$ containing 0.2 mol l^{-1} KCl solution) disappeared immediately. Therefore, CTA ions improve greatly the stability of Prussian blue in alkali solution. The improvement is assigned to hydrophobicity from CTA as counter ions in film. Because Prussian blue is very sensitive to hydroxy, it will be broken down when it is in touch with OH^- and form $Fe(OH)_3$ as follows:

$$KFeFe(CN)_6 + 3OH^- = Fe(OH)_3 + Fe(CN)_6^{4-} + K^+ \quad (7)$$

The hydrophobic CTA prevents PB from hydroxy and leads to relative stable voltammetric peaks.

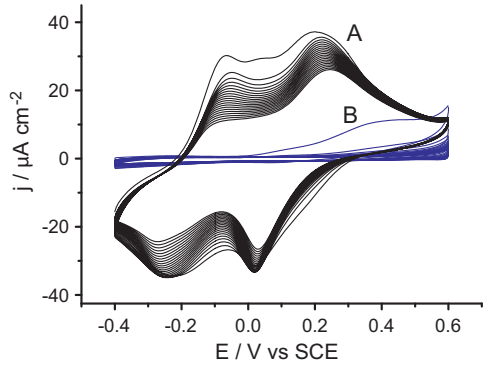

Fig. 13. Cyclic voltammograms of CTA-PB film (A) and Prussian blue (B) in 0.1 mol l^{-1} KOH solution at a scan rate of 50 mV s^{-1}.

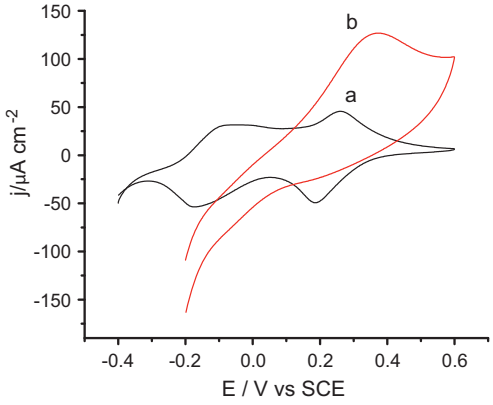

Fig. 14. Cyclic voltammetric curve (A) of CTA-PB electrode and electro-catalytic curve (B) of 6.50×10^{-5} mol l^{-1} hydrogen peroxide with 0.20 mol l^{-1} KCl supporting electrolyte at pH 7.40. Potential range: −0.40 to −0.60 V; scan rate: 50 mV s^{-1} .

3.10. Electrochemical response to hydrogen peroxide

Hydrogen peroxide is one of products that dioxygen is reduced by glucose in the presence of glucose-oxidase. Thus, the determination of the H_2O_2 concentration can characterize the glucose concentration indirectly. The voltammetric response of the CTA-PB electrode to hydrogen peroxide in pH 7.40 buffer solution is shown in Fig. 14. The results show that the oxidization peak current increases linearly with the concentration of hydrogen peroxide (Fig. 15) from 6.59×10^{-6} to 2.20×10^{-4} mol l^{-1} with $R = 0.99947$ ($n = 8$). The linear regression equation was I_p (mA) = 0.82949 + 0.00594C (μmol l^{-1}) with errors of $\pm 7.92833 \times 10^{-5}$ for the slope and ±0.01085 for the intercept

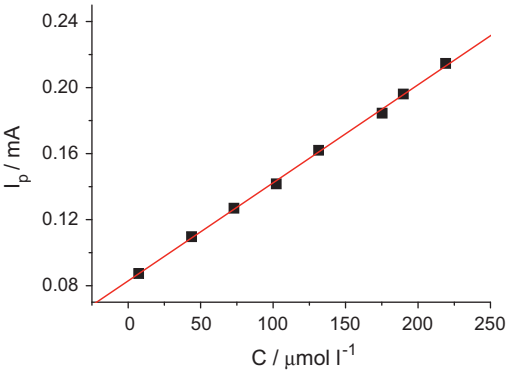

Fig. 15. Relationship between the concentration of hydrogen peroxide and the peak current.

with the detection limit of 1.46×10^{-6} mol l^{-1}. The dependence of peak currents on the concentration of hydrogen peroxide shows that CTA-PB may be applied in fabricating biosensors.

4. Conclusions

Prussian blue can be prepared by photoinducedly voltammetry from a single sodium nitroprusside. The formation mechanism is photochemical reaction first and subsequently electrochemical reaction. The cetyltrimethylammonium cations can enter into the channels of the Prussian blue as counter ions during voltammetric sweeps, as a result, CTAFeFe(CN)$_6$ is formed. The diffusion coefficients for CTA and potassium cations were estimated to be D_{CTA} 1.25×10^{-12} cm^2 s^{-1}, D_K 2.59×10^{-12} cm^2 s^{-1}, respectively. Because the peak current showed a linear dependence on hydrogen peroxide concentration from 6.59×10^{-6} to 2.20×10^{-4} mol l^{-1} with $R = 0.99947$, and the stability of CTAFeFe(CN)$_6$ film improves greatly in 0.1 mol l^{-1} KOH aqueous solution due to the hydrophobic effects of cetyltrimethylammonium, it is expected to find its application in aqueous neutral or weak alkali medium for biosensors.

Acknowledgements

This study was financially supported by Key Laboratory of Analytical Chemistry for Life Science, Ministry of Education (No. KLACLS 1013), the National Natural Science Foundation of China (No. 50973077, No. 21071107), the Creative Project of Postgraduate of Jiangsu Province (No. CX09S-049Z), China. We also thank Mr. Xian-He Liu from the Huaqiao University of China for the language check and Dr. Huang for the electroscope support of Public Center for Characterization and Test, Suzhou Institute of Nano-tech and Nano-bionics, Chinese Academy of Sciences.

Appendix A. Supplementary data

Supplementary data associated with this article can be found, in the online version, at doi:10.1016/j.electacta.2011.02.012.

References

[1] V.D. Neff, J. Electrochem. Soc. 125 (1978) 886.
[2] S. Sinh, B.D. Humphrey, A.B. Bocarsly, Inorg. Chem. 23 (1984) 203.
[3] K. Itaya, N. Shoji, I. Uchida, J. Am. Chem. Soc. 106 (1984) 3423.
[4] S.S. Kumar, J. Joseph, K.L. Phani, Chem. Mater. 19 (2007) 4722.
[5] L.D. Feng, J.M. Shen, X.H. Li, J.J. Zhu, J. Phys. Chem. C 112 (2008) 7617.
[6] G. Zhao, J.J. Feng, Q.L. Zhang, S.P. Li, H.Y. Chen, Chem. Mater. 17 (2005) 3154.
[7] J.D. Qiu, H.Z. Peng, R.P. Liang, J. Li, X.H. Xia, Langmuir 23 (2007) 2133.
[8] M. Orellana, P. Arriola, R. Del Río, R. Schrebler, R. Cordova, F. Scholz, H. Kahlert, J. Phys. Chem. B 109 (2005) 15483.
[9] D. Ellls, M. Eckhoff, V.D. Neff, J. Phys. Chem. 85 (1981) 1225.
[10] K.P. Rajan, V.D. Neff, J. Phys. Chem. 86 (1982) 4361.
[11] D.M. DeLongchamp, P.T. Hammond, Chem. Mater. 16 (2004) 4799.
[12] G. Gao, L. Xu, W. Wang, W. An, Y. Qiu, Z. Wang, E. Wang, J. Phys. Chem. B 109 (2005) 8948.
[13] P.R. Bueno, D. Giménez-Romero, C. Gabrielli, J.J. García-Jareño, H. Perrot, F. Vicente, J. Am. Chem. Soc. 128 (2006) 17146.
[14] J.J. García-Jareño, D. Giménez-Romero, F. Vicente, C. Gabrielli, M. Keddam, H. Perrot, J. Phys. Chem. B 107 (2003) 11321.
[15] D. Giménez-Romero, P.R. Bueno, C. Gabrielli, J.J. García-Jareño, H. Perrot, F. Vicente, J. Phys. Chem. B 110 (2006) 19352.
[16] D. Giménez-Romero, P.R. Bueno, J.J. García-Jareño, C. Gabrielli, H. Perrot, F. Vicente, J. Phys. Chem. B 110 (2006) 2715.
[17] P.J. Kulesza, M.A. Malik, M. Berrettoni, M. Giorgetti, S. Zamponi, R. Schmidt, R. Marassi, J. Phys. Chem. B 102 (1998) 1870.
[18] O. Sato, T. Iyoda, A. Fujishima, K. Hashimoto, Science 272 (1996) 704.
[19] V. Escax, A. Bleuzen, C. Cartier, F. Villain, A. Goujon, F. Varret, M. Verdaguer, J. Am. Chem. Soc. 123 (2001) 12536.
[20] M. Pyrasch, B. Tieke, Langmuir 17 (2001) 7706.
[21] D. Gimenez-Romero, J.J. García-Jareño, J. Agrisuelas, F. Vicente, J. Phys. Chem. C 112 (2008) 20099.
[22] D. Moscone, D. D'Ottavi, D. Compagnone, G. Palleschi, Anal. Chem. 73 (2001) 2529.
[23] Y. Lin, K. Liu, P. Yu, L. Xiang, X. Li, L. Mao, Anal. Chem. 79 (2007) 9577.

[24] D. Zhang, K. Zhang, Y.L. Yao, X.H. Xia, H.Y. Chen, Langmuir 20 (2004) 7303.
[25] W. Zhao, J.J. Xu, C.G. Shi, H.Y. Chen, Langmuir 21 (2005) 9630.
[26] H. Ohnuki, T. Saiki, A. Kusakari, H. Endo, M. Ichihara, M. Izumi, Langmuir 23 (2007) 4675.
[27] F. Ricci, G. Palleschi, Biosens. Bioelectron. 21 (2005) 389.
[28] N.A. Pchelintsev, A. Vakurov, P.A. Millner, Sens. Actuators B-Chem. 138 (2009) 461.
[29] C. Chen, Y. Fu, C. Xiang, Q. Xie, Q. Zhang, Y. Su, L. Wang, S. Yao, Biosens. Bioelectron. 24 (2009) 2726.
[30] L.C. Chen, K.C. Ho, Electrochim. Acta 46 (2001) 2151.
[31] H. Inaba, M. Iwaku, K. Nakase, H. Yasukawa, I. Seo, N. Oyama, Electrochim. Acta 40 (1995) 227.
[32] T.H. Kuo, C.Y. Hsu, K.M. Lee, K.C. Ho, Sol. Energy Mater Sol. Cells 93 (2009) 1755.
[33] B.T.T. Nguyen, J.Q. Ang, C.S. Toh, Electrochem. Commun. 11 (2009) 1861.
[34] N. Bagkar, C.A. Betty, P.A. Hassan, K. Kahali, J.R. Bellare, J.V. Yakhmi, Thin Solid Films 497 (2006) 259.
[35] K. Vasanthi, A.L. Xidis, V.D. Neff, Anal. Chim. Acta 239 (1990) 7.
[36] C. Gabrielli, P. Hémery, P. Liatsi, M. Masure, H. Perrot, J. Electrochem. Soc. 152 (2005) H219.
[37] M. Hermes, F. Scholz, J. Solid State Electrochem. 1 (1997) 21.
[38] R. Koncki, O.S. Wolfbeis, Sens. Actuators B-Chem. 51 (1998) 355.
[39] T. Lenarczuk, D. Wencel, S. Giab, R. Koncki, Anal. Chim. Acta 447 (2001) 23.
[40] U. Scharf, E.W. Grabner, Electrochim. Acta 41 (1996) 233.
[41] E. Bustons, J. Manríquez, G. Orozco, L.A. Godínez, Langmuir 21 (2005) 3013.
[42] A.A. Karyakin, E.E. Karyakina, L. Gorton, Electrochem. Commun. 1 (1999) 78.
[43] R. Vittal, M. Jayalakshmi, H. Gomathi, G. Prabhakara Rao, J. Electrochem. Soc. 146 (1999) 786.
[44] R. Vittal, H. Gomathi, G. Prabhakara Rao, Electrochim. Acta 45 (2000) 2083.
[45] S.M. Senthil Kumar, K. Chandrasekara Pillai, Electrochem. Commun. 8 (2006) 621.
[46] V. Hornok, I. Dékány, J. Colloid Interface Sci. 309 (2007) 176.
[47] S.M. Senthil Kumar, K. Chandrasekara Pillai, J. Electroanal. Chem. 589 (2006) 167.
[48] R. Vittal, H. Gomathi, J. Phys. Chem. B 106 (2002) 10135.
[49] R. Vittal, K.J. Kim, H. Gomathi, V. Yegnaraman, J. Phys. Chem. B 112 (2008) 1149.
[50] N.A. Kotov, I. Dékány, J.H. Fendler, J. Phys. Chem. 99 (1995) 13065.
[51] S.Q. Liu, J.J. Xu, H.Y. Chen, Electrochem. Commun. 4 (2002) 421.
[52] S.Q. Liu, H.Y. Chen, J. Electroanal. Chem. 528 (2002) 190.
[53] S.Q. Liu, Y. Chen, H.Y. Chen, J. Electroanal. Chem. 502 (2001) 197.
[54] A.G. Sharpe, The Chemistry of Cyano Complexes of the Transition Metals, Academic Press, London, UK, 1976, Ch. VII.
[55] G. Stochel, Z. Stasicka, Polyhedron 4 (1985) 1887.
[56] F. Roncardoli, R. van Eldik, J.A. Olabe, Inorg. Chem. 44 (2005) 2781.
[57] G. Stochel, R. van Eldik, Z. Stasicka, Inorg. Chem. 25 (1986) 3663.
[58] P.C. Ford, J. Bourassa, K. Miranda, B. Lee, I. Lorkovic, S. Boggs, S. Kudo, L. Laverman, Coord. Chem. Rev. 171 (1998) 185.
[59] K.S. Sidhu, W.R. Bansal, M. Sumanjit, J. Photochem. Photobiol. A: Chem. 65 (1992) 355.
[60] M.G. de Oliveira, J. Langley, A.J. Rest, J. Chem. Soc. Dalton Trans. (1995) 2013.
[61] Z. Stasicka, E. Wasielewska, Coord. Chem. Rev. 159 (1997) 271.
[62] P.R. Bueno, F.F. Ferreira, D. Giménez-Romero, G.O. Setti, R.C. Faria, C. Gabrielli, H. Perrot, J.J. Garcia-Jareño, F. Vicente, J. Phys. Chem. C 112 (2008) 13264.
[63] S.K.H. Kung, K.F. Hayes, Langmuir 9 (2003) 263.
[64] R. Birdwhistell, J. Chem. Educ. 69 (1992) 473.
[65] A.D. Bard, L.R. Faulkner, Electrochemical Methods: Fundamentals and Applications, 2nd ed., Wiley, NY, 2001, Ch. 6.
[66] R. Saliba, B. Agricole, C. Mingotaud, S. Ravaine, J. Phys. Chem. B 103 (1999) 9712.